

Hydrothermal synthesis and characterization of the first 1-D indiumphosphate chain $\text{In}_2(\text{HPO}_4)_2(\text{H}_2\text{PO}_4)_2\text{F}_2 \cdot \text{C}_4\text{N}_2\text{H}_{12}$, a precursor for high dimensional structures

Chao Chen^a, Zhuo Yi^a, Minghui Bi^a, Yunling Liu^a, Chunyu Wang^b,
Li Liu^a, Zan Zhao^a, Wenqin Pang^{a,*}

^aState Key Laboratory of Inorganic Synthesis and Preparative Chemistry, College of Chemistry, Jilin University, Changchun 130012, P.R. China

^bKey Lab for Supramolecular Structure and Materials of Ministry of Education, Jilin University, Changchun 130012, P.R. China

Received 22 November 2005; received in revised form 22 January 2006; accepted 28 January 2006

Available online 9 March 2006

Abstract

The first one-dimensional (1-D) indiumphosphate chain, $\text{In}_2(\text{HPO}_4)_2(\text{H}_2\text{PO}_4)_2\text{F}_2 \cdot \text{C}_4\text{N}_2\text{H}_{12}$ (**1**), has been hydrothermally prepared using piperazine (PIP) as a template. The structure consists of infinite chains of *trans,trans*-corners-sharing InO_4F_2 octahedra with the adjacent octahedra being bridged by tetrahedral $\text{PO}_3(\text{OH})$ and $\text{PO}_2(\text{OH})_2$ units, which are H-bonded with amine groups of the organic cations. Interestingly, this macroanionic chain $\text{InP}_2\text{O}_8\text{H}_3\text{F}^-$ is similar to that found in the mineral tancoite-like chains and has potential to further set up higher-dimensional networks. On heating **1** in the presence of additional phosphoric acid at 180 °C under hydrothermal condition, compound **2**, $\text{In}_2(\text{OH})(\text{H}_2\text{O})(\text{PO}_4)_2 \cdot \text{H}_3\text{O} \cdot \text{H}_2\text{O}$, possessed a 3-D structure building from the repetition of a secondary building unit is obtained. When **1** is heated with additional PIP, an unknown phase, compound **3** is formed. Finally, on treatment with another amine, such as diethylenetriamine or 1,4-diaminobutane, at 180 °C, **1**, as a precursor, can convert into a previously known 3-D framework structure with 16-membered ring compound **4**. Compounds **1** and **2** are determined by single-crystal X-ray diffraction. Furthermore, **1** is characterized by X-ray powder diffraction, IR spectroscopy, inductively coupled plasma analysis, thermogravimetric analysis and differential thermal analysis.

© 2006 Elsevier Inc. All rights reserved.

Keywords: Indiumphosphate; Hydrothermal synthesis; Precursor; Transformation

1. Introduction

Open-framework structures, especially those of metal phosphates, have been of great interest in the past few years because of their potential applications in catalysis and separation processes, and also due to the fascinating structural features exhibited by them [1–7]. Recently, the research for the detailed understanding of how microporous metal phosphates are formed is very intense because it will enable the rational design of new materials with properties required for a particular use [8]. Some postulation of reaction mechanism has taken place based on numerous structural data of metal phosphates. For

example, Ozin and co-workers [9] proposed a self-assembly model for the transformation of aluminophosphates. Férey and co-workers [10,11] also described the concept of building units to understand the formation of gallium- and titanium-phosphates. Carefully studying the transformation of different dimensional zinc phosphates, Rao and co-workers [12,13] believed that the zero-dimensional (0-D) monomers, comprising four-membered rings, are the basic structural units of the zinc phosphates and after an optimal precursor state, such as the ladder structure, to construct into high-dimensional structure. However, compared with the researches for the structural transformation mechanism on MPOs ($M = \text{Al}, \text{Ga}$ and Zn) families with the M of 4-, 5- and 6-coordination (or mixtures), the research for that on indiumphosphates is rarely documented, though it might be more readily understood because only rigid

*Corresponding author. Fax: +86 431 516 8624.

E-mail address: wqpang@mail.jlu.edu.cn (W. Pang).

octahedral coordination of indium is expected in InPO. It may be due to the fact that there are only 3-D open-framework InPOs with In/P ratios of 1/2 [14,15], 2/3 [16], 1/1 [17,18], 9/8 [19], 5/4 [20], 6.8/8 [21], and 2-D layers with In/P ratios of 1/3 [22], 1/2 [23–25], 4/7 [26], 1/1 [20] up to now. The low-dimensional indiumphosphate, such as 1-D chains and 0-D monomer, has not yet been discovered, which results that there is not sufficient data to systematically study the structural transformation mechanism. Our scientific research group has delved into the synthesis of group 13 phosphates in last 10 years. Herein, a linear fluorinated indiumphosphate (**1**) was successfully synthesized. Besides, for understanding the formation mechanisms of the microporous indiumphosphates, the dimensional transformation using compound **1** as a starting material was studied. Under different reaction conditions, compounds **2**, **3** and **4** with different structures were obtained, in which **1** plays diversity of roles during transformation.

2. Experimental

2.1. Synthesis and characterization

Compound **1** was synthesized by a hydrothermal method from a mixture of indiumnitrate ($\text{In}(\text{NO}_3)_3 \cdot 4.5\text{H}_2\text{O}$, Shanghai Reagent Plant, 99.5%), phosphoric acid (Beijing Chemical Plant, 85 wt%), piperazine (PIP, ACROS), hydrofluoric acid (Beijing Chemical Plant, 40%) and distilled water with the molar ratio of $\text{In}(\text{NO}_3)_3 \cdot 4.5\text{H}_2\text{O} : 4.0 \text{H}_3\text{PO}_4 : 2.0 \text{PIP} : 7.0 \text{HF} : 555 \text{H}_2\text{O}$. Typically, indiumnitrate was first dispersed into 9 mL of H_2O with stirring, then 0.36 mL of H_3PO_4 and 0.3 mL HF were added successively to form a clear solution. Finally, 0.28 mL of PIP was added dropwise under vigorous stirring. The white gel, thus, formed was stirred until homogeneous. The final mixture was sealed in a Teflon-lined stainless-steel autoclave and heated at 180 °C for 10 days under autogenous pressure. The product consisting of colorless platelet-shaped crystals was separated by sonication, further washed with distilled water and dried at room temperature.

The transformations were performed under hydrothermal conditions. In a typical procedure, a 0.1 g sample of **1** (grinded previously), 0.12 mL H_3PO_4 and 2 mL H_2O were sealed in a Teflon-lined stainless-steel autoclave and heated at 180 °C for 6 days. The crystals of compound **2** (in about 50% yield based on In source) were obtained, which separated by sonication, further washed with water, and dried at room temperature. While on heating 0.1 g sample of **1**, 0.09 g PIP and 2 mL H_2O at 160 °C for 24 h, an unknown phase with white powder (denoted **3**) was obtained. On heating 0.1 g compound **1**, 0.12 mL diethylenetriamine (DETA) (or 0.10 mL 1,4-diaminobutane (1,4-DBA)) and 2 mL H_2O at 160 °C for 6 days, the powder of **4** was yielded, which possesses the previously known 3-D framework structure with 16-membered ring proved by powder X-ray diffraction (XRD) [21].

Powder XRD data were collected on a Siemens D5005 diffractometer with $\text{CuK}\alpha$ radiation ($\lambda = 1.5418 \text{ \AA}$). The step size was 0.02° and the count time was 2 s. The elemental analyses were performed on a Perkin-Elmer 2400 LSII element analyzer. Inductively couple plasma (ICP) analyses were carried out on a Perkin-Elmer Optima 3300 DV ICP instrument. A Perkin-Elmer DTA 1700 differential thermal analyzer was used to obtain the differential thermal analysis (DTA), and a Perkin-Elmer TGA 7 thermogravimetric analyzer was used to obtain thermogravimetric analysis (TGA) curves in an atmospheric environment with a heating ratio of $10^\circ\text{C min}^{-1}$. The IR spectrum was recorded on a Nicolet Impact 410 FT-IR spectrometer within the $400\text{--}4000 \text{ cm}^{-1}$ using KBr pellets.

2.2. Determination of crystal structure

A suitable crystal of **1** and **2** was mounted on a glass fiber on a Bruker-AXS Smart CCD diffractometer equipped with a normal-focus, 2.4 kW sealed tube X-ray source (graphite-monochromated $\text{MoK}\alpha$ radiation, $\lambda = 0.71073 \text{ \AA}$). A total of 5974 reflections for **1** and 9497 reflections for **2** were collected at 293 K with 2149 and 2286 unique reflections, respectively ($R_{\text{int } 1} = 0.0647$ and $R_{\text{int } 2} = 0.0313$). Data processing was accomplished with the SAINT processing program. The structures of two compounds were all solved by direct methods and refined by full-matrix least-squares on F^2 using SHELXTL Version 5.1 [29]. The indium and phosphorus atoms were first located, and the oxygen, fluorine, carbon and nitrogen atoms were found in the final difference Fourier maps. Then the nonhydrogen atoms were refined anisotropically. Finally, the hydrogen atoms were initially located from difference Fourier maps and for the final refinement were placed geometrically. The detailed crystallographic data of the two compounds are listed in Table 1. The atomic coordinates and equivalent isotropic displacement parameters are listed in Table 2 and 3, respectively.

3. Results and discussion

3.1. Synthesis and characterization

The experimental XRD patterns of **1** and **2** were entirely consistent with that simulated on the basis of the single-crystal structures, which showed that the products were monophasic. The diffraction peak positions of powder XRD characterization of compound **3** were different from those reported indiumphosphates suggested **3** might be a new phase. The experimental XRD pattern of **4** and the simulated pattern based on the crystallographic data reported by Thirumurugan and Natarajan [21] present in Fig. 1(f) and (g), which suggested **4** is a previously known 3-D framework structure with 16-membered ring compound. The elemental analysis and ICP analysis results of four compounds indicated that compound **1** contained 6.35 wt% C, 3.78 wt% N, 31.25 wt% In and 16.85 wt% P, in

Table 1
Crystal data and structure refinement for **1** and **2**

Empirical formula	In ₂ (HPO ₄) ₂ (H ₂ PO ₄) ₂ F ₂ · C ₄ N ₂ H ₁₂	In ₂ (OH)(H ₂ O)(PO ₄) · H ₃ O · H ₂ O
Formula weight	741.72	491.64
Temperature (K)	293(2)	293(2)
Wavelength (Å)	0.71073	0.71073
Crystal system	Orthorhombic	Monoclinic
Space group	<i>Pbcn</i>	<i>P2(1)/n</i>
Unit cell dimensions	<i>a</i> = 16.987(10) Å <i>b</i> = 7.519(3) Å <i>c</i> = 13.916(8) Å	<i>a</i> = 10.040(2) Å <i>b</i> = 9.885(2) Å <i>c</i> = 10.323(2) Å <i>β</i> = 102.93(3)°
Volume (Å ³)	1777.5(15)	998.6(3)
Z	4	4
Density (calculated) (Mg/m ³)	2.772	3.137
Absorption coefficient (mm ⁻¹)	3.065	4.978
<i>F</i> (000)	1440	884
Crystal size (mm ³)	0.200 × 0.100 × 0.050	0.200 × 0.200 × 0.200
<i>θ</i> range for data collection (deg.)	2.40–28.95	3.21–27.47
Limiting indices	−6 ≤ <i>h</i> ≤ 22 −9 ≤ <i>k</i> ≤ 10 −14 ≤ <i>l</i> ≤ 15	−13 ≤ <i>h</i> ≤ 12 −12 ≤ <i>k</i> ≤ 12 −13 ≤ <i>l</i> ≤ 12
Reflections collected/unique	5974/2149 [<i>R</i> _{int} = 0.0647]	9497/2286 [<i>R</i> _{int} = 0.0313]
Data/restraints/parameters	2149/0/134	2286/0/172
Goodness-of-fit on <i>F</i> ²	0.929	1.024
Final <i>R</i> indices [<i>I</i> > 2σ(<i>I</i>)] ^a	<i>R</i> ₁ = 0.0363, <i>wR</i> ₂ = 0.0785	<i>R</i> ₁ = 0.0303, <i>wR</i> ₂ = 0.0923
<i>R</i> indices (all data)	<i>R</i> ₁ = 0.0686, <i>wR</i> ₂ = 0.0897	<i>R</i> ₁ = 0.0343, <i>wR</i> ₂ = 0.0990
Largest diffraction peak and hole (e Å ⁻³)	1.104 and −0.792	1.149 and −2.087

$$^a R_1 = \sum ||F_o| - |F_c|| / \sum |F_o| \text{ and } wR_2 = [\sum [w(F_o^2 - F_c^2)^2] / \sum [w(F_o^2)^2]]^{1/2}.$$

Table 2
Atomic coordinates (× 10⁴) and equivalent isotropic displacement parameters (Å² × 10³) for **1**

Atom	<i>x</i>	<i>y</i>	<i>z</i>	<i>U</i> (eq.) ^a
In(1)	2519(1)	−257(1)	2439(1)	13(1)
P(2)	3719(1)	2172(2)	3790(1)	14(1)
P(1)	3438(1)	2254(2)	853(1)	15(1)
F(1)	3070(2)	−2779(4)	2421(2)	18(1)
O(8)	3736(3)	2489(5)	4893(3)	24(1)
O(7)	4270(2)	2381(5)	424(3)	23(1)
O(6)	2894(2)	1868(6)	−15(3)	24(1)
O(5)	3231(2)	477(5)	3615(3)	19(1)
O(4)	3416(2)	770(5)	1569(3)	20(1)
O(3)	4560(2)	1940(5)	3496(3)	22(1)
O(2)	1648(2)	−1224(5)	3330(3)	24(1)
O(1)	1831(2)	−1005(5)	1248(3)	23(1)
N(2)	5136(8)	4046(19)	8299(10)	37(4)
C(2)	4880(10)	2130(20)	8379(13)	36(4)
N(1)	4859(7)	1911(16)	6640(9)	23(3)
C(1)	5154(5)	1138(10)	7506(10)	6(2)
C(4)	4846(5)	4821(11)	7412(10)	9(2)
C(3)	5086(9)	3740(19)	6532(11)	26(4)

^a *U* (eq.) is defined as one-third of the trace of the orthogonalized *U*_{*ij*} tensor.

Table 3
Atomic coordinates (× 10⁴) and equivalent isotropic displacement parameters (Å² × 10³) for **2**

Atom	<i>x</i>	<i>y</i>	<i>z</i>	<i>U</i> (eq.) ^a
In(1)	3848(1)	10,495(1)	−1312(1)	8(1)
In(2)	975(1)	7656(1)	3117(1)	8(1)
P(2)	2887(1)	9609(1)	1421(1)	9(1)
P(1)	2902(1)	8297(1)	−3746(1)	9(1)
O(7)	2779(4)	9723(4)	−3143(4)	12(1)
O(6)	2568(4)	9790(4)	−108(4)	14(1)
O(5)	−602(4)	7133(4)	1503(4)	15(1)
O(4)	1850(4)	8614(4)	1710(4)	16(1)
O(3)	2929(5)	12,339(4)	−1921(5)	18(1)
O(2)	2369(4)	8412(4)	4758(4)	15(1)
O(1)	−97(5)	9576(5)	3307(5)	24(1)
O(11)	5050(4)	11,451(4)	604(4)	10(1)
O(10)	2255(4)	5983(4)	2928(4)	14(1)
O(9)	5658(4)	10,944(4)	−1944(4)	12(1)
OW2	10,027(6)	8008(6)	8997(6)	37(1)
OW1	1700(5)	1488(5)	4633(5)	26(1)

^a *U* (eq.) is defined as one-third of the trace of the orthogonalized *U*_{*ij*} tensor.

good agreement with the values (calcd.: 6.47, 3.77, 30.96 and 16.72 wt% of C, N, In and P, respectively) based on the single-crystal structure formula In₂(HPO₄)₂(H₂PO₄)₂F₂ · C₄N₂H₁₂; compound **2** contained 44.82 wt% In and 12.6 wt% P (calcd.: 46.72 wt% In; 12.65 wt% P); compound **3** contained

29.25 wt% In, 16.84 wt% P, 6.55 wt% C, 3.90 wt% N and 2.12 wt% F; compound **4** (using DETA as a template) contained 5.88 wt% C, 6.96 wt% N and 6.50 wt% F. The TGA of **1** shows that the weight loss of the compound is ca. 16.3 wt% from 240 to 750 °C, corresponding to the decomposition of the PIP template (calcd.: 11.86 wt%) and

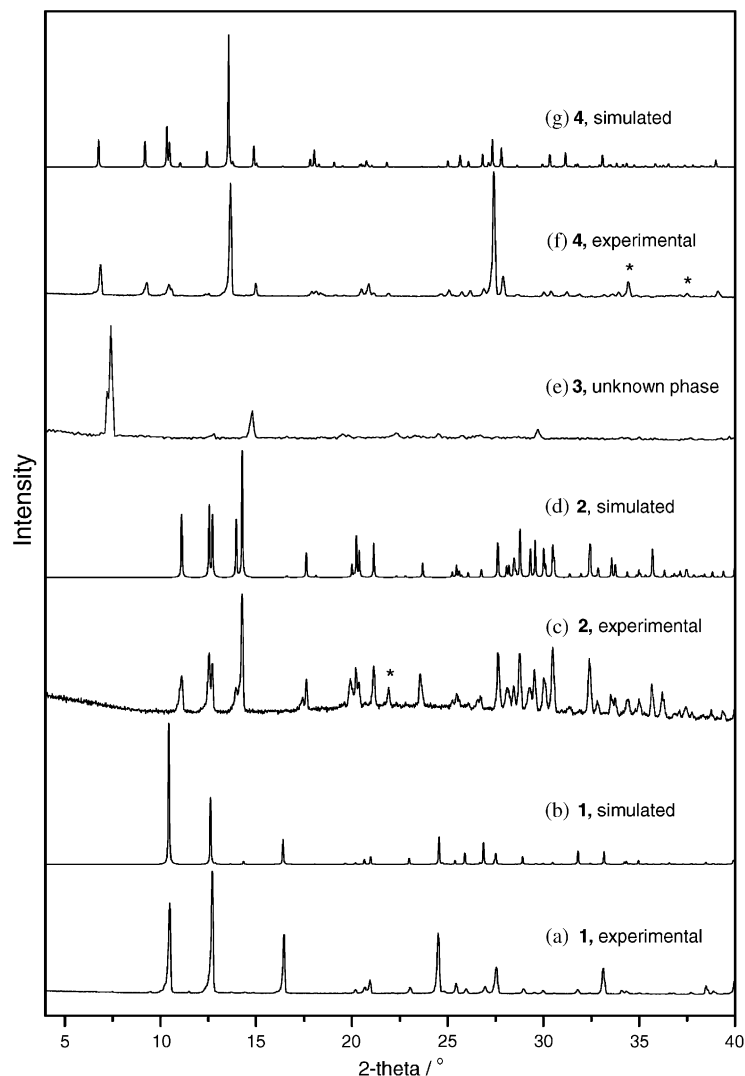


Fig. 1. Experimental and simulated powder XRD patterns of the various phases (asterisk denotes an unidentified phase): (a) experimental powder XRD patterns of **1**; (b) simulated powder XRD patterns of **1**; (c) experimental powder XRD patterns of **2** (on heating **1** and additional H_3PO_4 at 180°C for 6 days); (d) simulated powder XRD patterns of **2**; (e) experimental powder XRD patterns of **3** (on heating **1** and additional PIP at 160°C for 24 h); (f) experimental powder XRD patterns of **4** (on heating **1** and TETA at 160°C for 6 days); (g) simulated powder XRD patterns of **4** (based on the crystallographic data in Ref. [21]).

dehydration of the compound (calcd.: 4.85 wt%), and the weight loss of 5.6 wt% at $750\text{--}950^\circ\text{C}$ is consistent with removal of HF (calcd.: 5.39 wt%). The DTA curve of **1** exhibits two endothermic and one exothermic peak at ca. 400, 780 and 920°C , corresponding to the departure of the template, dehydroxylation and removal of HF. IR spectrum of the sample **1** shows that the broadbands in $3500\text{--}3000\text{ cm}^{-1}$ are typically attributed to O–H and N–H bands. The bands at 1706, 1610, 1394, 1210 and 1102 cm^{-1} confirm the presence of PIP cations. Additional In–O and P–O bands are observed at 981, 920, 602 and 506 cm^{-1} .

3.2. Description of the structure

An ORTEP drawing of the asymmetric unit for **1** is shown in Fig. 2(a). It contains a crystallographically

distinct In atom, one F atom and two different P atoms. In atom is octahedrally coordinated, sharing four vertex oxygen atoms with adjacent P atoms ($\text{In}\text{--}\text{O}_{\text{av}} = 2.092\text{ \AA}$) and two bridging F atoms with another In atoms ($\text{In}\text{--}\text{F}_{\text{av}} = 2.115\text{ \AA}$). The F–In–F bond angle for two fluorine atoms in a *trans* position is close to 180° (F(1)–In(1)–F(1A) bond angle is $177.657(12)^\circ$). The tetrahedral P(1) atom shares two oxygen atoms with adjacent In atoms, leaving the other two oxygen atoms as terminal P–OH groups with P–O bond lengths of 1.547(4) and 1.537(4) Å. P(2) atom also shares two oxygen atoms with adjacent In atoms, but the other two oxygen atoms are terminal P=O/P–OH groups ($d_{\text{P}(2)\text{--}\text{O}(3)} = 1.496(4)\text{ \AA}$) and P–OH group ($d_{\text{P}(2)\text{--}\text{O}(8)} = 1.553(4)\text{ \AA}$). These results are close to those observed previously in indium phosphates [14–26].

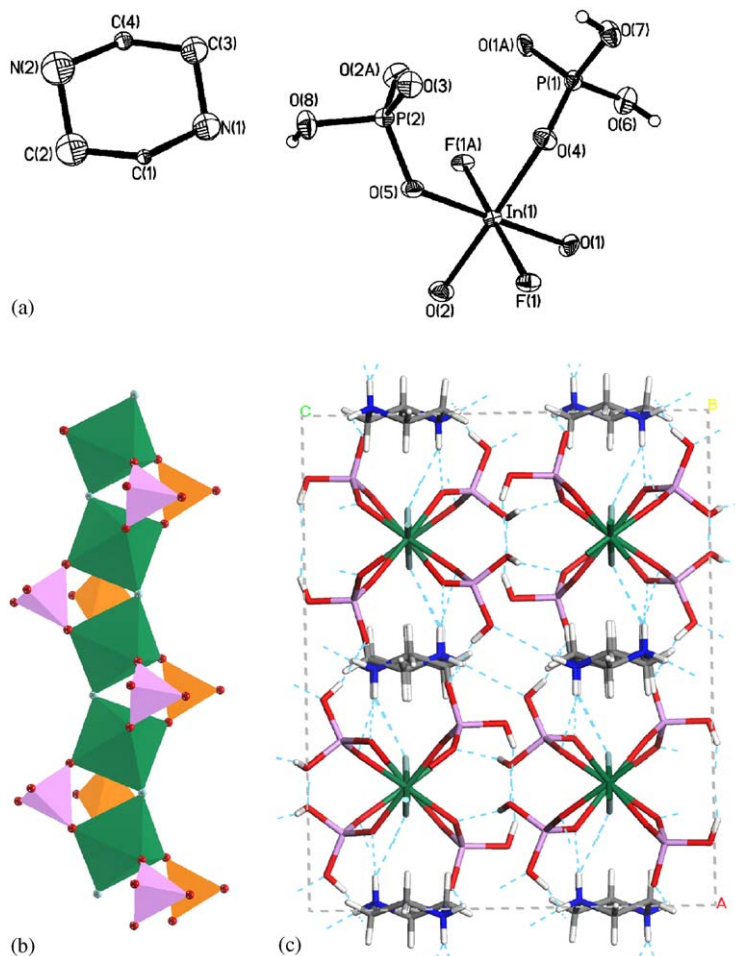


Fig. 2. (a) ORTEP view of the structure of **1** showing the atom-labeling scheme (50% thermal ellipsoids); (b) polyhedral view of the chain in **1** running parallel to the [010] direction; (c) the hydrogen-bonding interactions among the inorganic chains and the piperazine molecules (viewed along the *b*-axis).

The structure consists of infinite macroanionic chains of empirical formula $[\text{In}_2(\text{HPO}_4)_2(\text{H}_2\text{PO}_4)_2\text{F}_2]^{2-}$ separated by PIP cations. Fig. 2(b) shows the polyhedral view of the chains running parallel to the [010] direction. The InO_4F_2 octahedral chains are linked in a *trans-trans* configuration, and adjacent octahedra are bridged by HPO_4 and H_2PO_4 groups. There exist as similar 1-D chain structure, such as the natural mineral of tancoite and other metal phosphates [30–33], as the title compound. The difference is that there exists $-\text{M}-\text{X}-\text{M}-$ ($\text{M} = \text{Al}$ or Ga , $\text{X} = \text{OH}$ or F) infinite linkages in those chains instead of $-\text{In}-\text{F}-\text{In}-$ linkages in that of **1**. The infinite chains are held together by extensive hydrogen bonds among the inorganic chains and the organic amines (as shown in Fig. 2(c)).

Single-crystal XRD analysis reveals that compound **2** is isostructural with that of well-known leucophosphate mineral [34] and an indiumphosphate (denoted compound **5**) reported by Koh et al. [35]. The cations as the charge-compensating ions of **2** are a protonated water and a neutral water, whereas that of **5** corresponds to NH_4^+ and water. It results the framework of **2** is slightly deformed than that of **5**. Compound **2** possesses a 3-D open-

framework structure which may be understood in terms of an unusual secondary building unit (SBU), the octamer, with formula of $\text{In}_4(\text{H}_2\text{O})_2(\text{OH})_2(\text{PO}_4)_4$. From Fig. 3(b), we can see the SBU consists of a central pair of edge-sharing $\text{In}(1)(\text{OH})\text{O}_5$ octahedra connected via O(11) atoms to which two additional $\text{In}(2)(\text{H}_2\text{O})(\text{OH})\text{O}_4$ octahedra are attached by corner sharing also via O(11), forming a tetramer. Thus, O(11) is coordinated to three In atoms and also bonded to one H as suggested by XRD results, so having 4-coordination, which is rarely documented in indiumphosphates. Additionally, both types of InO_6 polyhedra have far from regular octahedral coordination, the distortion being greater in $\text{In}(1)\text{O}_6$ edge-sharing units ($\text{In}(1)-\text{O}$ bond distances are in the range of 2.076(4)–2.280(4) Å, and 2.080(4)–2.212(4) Å for $\text{In}(2)-\text{O}$ bonds). Then, the PO_4 tetrahedra cap the tetramer by the bridging oxygen atoms to generate the octamer. These octamers further fuse together via the PO_4 groups to construct into the 3-D framework with eight-ring channels running along the *b*-axis. The H_3O^+ cations and molecular H_2O are trapped in the 8-MR channels and interact with the oxygens attached to the framework through H bonds.

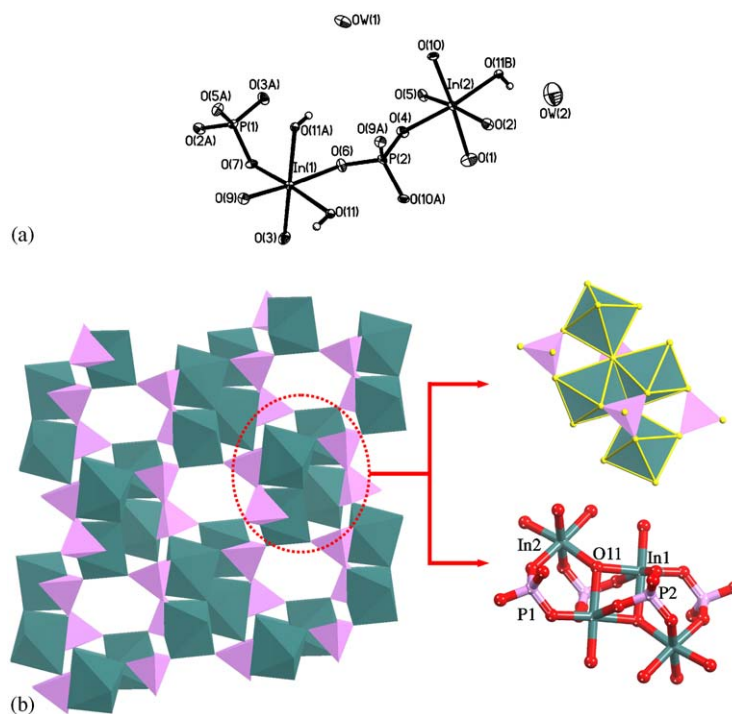


Fig. 3. (a) ORTEP view of the structure of **2** showing the atom-labeling scheme (50% thermal ellipsoids); (b) the description of the structural fashion of **2**: polyhedral representation of the 3-D structure along the *b*-axis for **2**. Note the unusual SBU, the octamer, with formula of $\text{In}_4(\text{H}_2\text{O})_2(\text{OH})_2(\text{PO}_4)_4$, constructed into the structure.

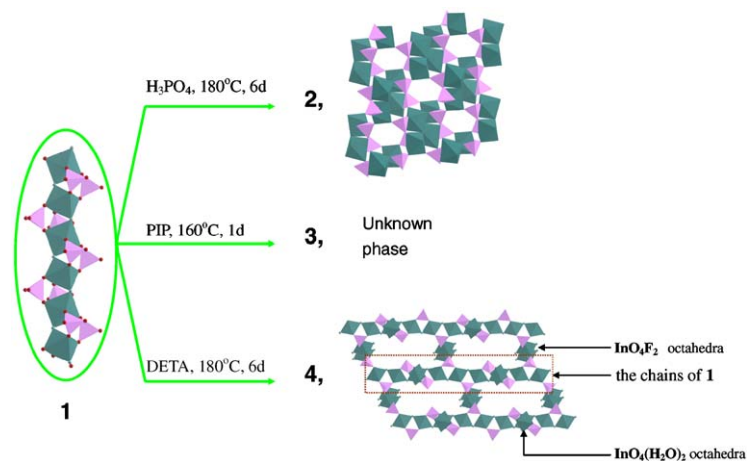


Fig. 4. Schematic of the transformation from **1** to the high-dimensional structures under different reaction conditions.

It is worthy to note that the feature of SBU in **2** is rare among the numerous indium phosphates. In $\text{In}_4(\text{H}_2\text{O})_2(\text{OH})_2(\text{PO}_4)_4$ octamer, three InO_6 octahedra are bridged by sharing vertices and edges in which the geometric tension around In is minimized. It leads to the enhancing structural rigidity and stability. So utilization of the SBUs as basic units may provide an approach to construct into the stable, large-pore open-framework structure. In fact, the SBU already presents in the iron (or gallium) phosphate analog with large tunnels containing 20-ring windows [36,37].

Some extended researches are underway to obtain large pore structure based on such type of SBU.

3.3. Transformation behavior of **1**

Given the interest in the conversion of low-dimensional phosphates to those with structures of higher dimensionality in relation to understanding the crystallization mechanism, we investigated the transformation behavior of **1** under hydrothermal conditions. As shown in Fig. 4, on heating **1**

in the presence of additional PIP at 160 °C in water for relatively short periods (24 h), a new phase (**3**), proved by powder XRD, was yielded, suggesting that the chain may transformed to another structure. But this phase could not be further characterized since we could not isolate a single crystal. While on heating **1** and additional H₃PO₄ at 180 °C in water, compound **2**, with 3-D framework structure, was obtained. However, noting that the distinct difference between the structures of **1** and **2**, plus there is no F traced in compound **2**, it suggests that **1** only plays a role of providing sole source of reactants, other than as a precursor or intermediate material proposed by Rao and Férey for the transformation of ZnPOs and GaPOs. Finally, when heated **1** in the presence of another amine, such as TETA or 1,4-DBA at 180 °C, **1** could convert to a previously known compound, [NH₃(CH₂)₂NH₂(CH₂)₂NH₃]₂[NH₂(CH₂)₂NH₂(CH₂)₂NH₂][In_{6.8}F₈(H₂O)(PO₄)₄(HPO₄)₄]·H₂O, **4**, described by Thirumurugan and Natarajan [21]. Interestingly, **4** possesses a 3-D framework structure with 16-membered ring, which can be understood as constructed from the chains of **1** cross-linked by InO₄(H₂O)₂ and InO₄F₂ octahedra. So, **1** probably plays two roles, dissolving in solution acting as In source of reactants and as the precursor for constructing into the structure of **4**. Thus, through condensations of the terminal P=O and P-OH groups protruding from the chains and InO₄(H₂O)₂ and InO₄F₂ groups dissolved in the solution, **1** could further form higher-dimensional framework compounds. It is noteworthy that the formation of **4** is sensitive to the additional organic amine. Compound **1** could not be transformed to compound **4** without additional DETA or 1,4-DBA. It suggests that DETA or 1,4-DBA is more suitable for templating the formation of **4** compared to PIP.

4. Conclusions

Templated by PIP, the first 1-D indiumphosphate chain, In₂(HPO₄)₂(H₂PO₄)₂F₂·C₄N₂H₁₂ (**1**), has been prepared by hydrothermal technique. Furthermore, the chain is similar to the mineral tancoite chain and presents a potential ability to further set up higher-dimensional networks. Careful investigation clearly demonstrated that compound **1** could transform into compounds **2**, **3** and **4** with different structures under different conditions. The transformed roles of **1** were discussed, and it proved a possible way to rationally design and synthesize the target metal phosphates.

5. Supporting information and structure details

Crystallographic data for the structure reported in this paper in the form of CIF file have been deposited with the Cambridge Crystallographic Data Centre as supplementary publication no. CCDC-266728 for **1**. Copies of the data can be obtained free of charge on application to CCDC, 12 Union Road, Cambridge CB2 1EZ, UK (Fax: +44 1223 336 033; E-mail: deposit@ccdc.cam.ac.uk).

Acknowledgments

We are grateful to the financial support of the Ministry of Science and Technology of China through the State Basic Research Project (G200077507) and the National Natural Science Foundation of China (20233030).

Appendix A. Supplementary materials

Supplementary data associated with this article can be found in the online version at [doi:10.1016/j.jssc.2006.01.074](https://doi.org/10.1016/j.jssc.2006.01.074).

References

- [1] A.K. Cheetham, G. Férey, T. Loiseau, *Angew. Chem. Int. Ed.* 38 (1999) 3268 (and references therein).
- [2] S.H. Feng, R.R. Xu, *Acc. Chem. Res.* 34 (2001) 239.
- [3] S.T. Wilson, B.M. Lok, C.A. Messian, T.R. Cannan, E.M. Flanigen, *J. Am. Chem. Soc.* 104 (1982) 1146.
- [4] M. Esternam, L.B. McCusker, C. Baerlocher, A. Merrouche, H. Kessler, *Nature* 352 (1991) 320.
- [5] W.T.A. Harrison, T.E. Martin, T.E. Gier, G.D. Stucky, *J. Mater. Chem.* 2 (1992) 175.
- [6] K.H. Lii, Y.F. Huang, V. Zima, C.Y. Huang, H.M. Lin, Y.C. Jiang, F.L. Liao, S.L. Wang, *Chem. Mater.* 10 (1998) 2599 (and references therein).
- [7] Y. Zhang, A. Clearfield, R.C. Haushalter, *Chem. Mater.* 7 (1995) 1221.
- [8] A.K. Cheetham, C.F. Mellot, *Chem. Mater.* 9 (1997) 2269.
- [9] S. Oliver, A. Kuperman, G.A. Ozin, *Angew. Chem. Int. Ed.* 37 (1998) 47.
- [10] G. Férey, *Chem. Mater.* 13 (2001) 3084.
- [11] C. Serre, F. Tanlèlle, G. Férey, *Chem. Commun.* (2003) 2755.
- [12] C.N.R. Rao, S. Natarajan, A. Choudhury, S. Neeraj, A.A. Ayi, *Acc. Chem. Res.* 34 (2001) 80.
- [13] A. Choudhury, S. Neeraj, S. Natarajan, C.N.R. Rao, *J. Mater. Chem.* 12 (2002) 1044.
- [14] S.S. Dhingra, R.C. Haushalter, *J. Chem. Soc. Chem. Commun.* (1993) 1665.
- [15] C. Chen, Z. Yi, H. Ding, G.H. Li, M.H. Bi, Y.L. Yang, S.G. Li, W.S. Li, W.Q. Pang, *Microporous Mesoporous Mater.* 83 (2005) 301.
- [16] S.S. Dhingra, R.C. Haushalter, *J. Solid State Chem.* 112 (1994) 96.
- [17] Z. Yi, Y.L. Yang, K.K. Huang, G.H. Li, C. Chen, W. Wang, Y.L. Liu, W.Q. Pang, *J. Solid State Chem.* 177 (2004) 4073.
- [18] Y. Xu, L.L. Koh, L.H. An, R.R. Xu, S.L. Qiu, *J. Solid State Chem.* 117 (1995) 373.
- [19] I.D. Williams, J.H. Yu, H.B. Du, J.S. Chen, W.Q. Pang, *Chem. Mater.* 10 (1998) 773.
- [20] H.B. Du, J.S. Chen, W.Q. Pang, J.H. Yu, I.D. Williams, *Chem. Commun.* (1997) 781.
- [21] A. Thirumurugan, S. Natarajan, *Dalton Trans.* (2003) 3387.
- [22] A.M. Chippindale, S.J. Brech, *Chem. Commun.* (1996) 2781.
- [23] K.-H. Lii, Y.-F. Huang, *Inorg. Chem.* 38 (1999) 1348.
- [24] J.H. Yu, H.H.-Y. Sung, I.D. Williams, *J. Solid State Chem.* 142 (1999) 241.
- [25] Y. Du, J.H. Yu, Y. Wang, Q.H. Pan, Y.C. Zou, R.R. Xu, *J. Solid State Chem.* 177 (2004) 3032.
- [26] A.M. Chippindale, S.J. Brech, A.R. Cowley, W.M. Simpson, *Chem. Mater.* 8 (1996) 2259.
- [29] SMART and SAINT (Software Packages), Siemens Analytical X-ray Instruments Inc., Madison, WI, 1996.
- [30] F.C. Hawthorne, *Acta Cryst. B* 50 (1994) 481.

- [31] M.P. Attfield, R.E. Morris, I. Burshtein, C.F. Campana, A.K. Cheetham, *J. Solid State Chem.* 118 (1995) 412.
- [32] W.F. Yan, J.H. Yu, Z. Shi, Y. Wang, Y.C. Zou, R.R. Xu, *J. Solid State Chem.* 161 (2001) 259.
- [33] R.I. Walton, F. Millange, D. O'Hare, *Chem. Mater.* 12 (2000) 1977.
- [34] P.B. Moore, *Am. Mineral.* 57 (1972) 397.
- [35] L.L. Koh, Y. Xu, H.B. Du, W.Q. Pang, *Stud. Surf. Sci. Catal.* 105 (1997) 373.
- [36] K.-H. Lii, Y.-H. Huang, *Chem. Commun.* (1997) 839.
- [37] A.M. Chippindale, K.J. Peacock, A.R. Cowley, *J. Solid State Chem.* 145 (1999) 379.